Catena 187 (2020) 104414

Contents lists available at ScienceDirect

Catena

journal homepage: www.elsevier.com/locate/catena

Organic carbon burial and sources in soils of coastal mudflat and mangrove ecosystems

Sigit D. Sasmito[a,b,*], Yakov Kuzyakov[c,d,e,f], Ali Arman Lubis[g], Daniel Murdiyarso[b,h], Lindsay B. Hutley[a], Samsul Bachri[i], Daniel A. Friess[j], Christopher Martius[k], Nils Borchard[b,l]

[a] Research Institute for the Environment and Livelihoods (RIEL), Charles Darwin University, Darwin, NT 0810, Australia
[b] Center for International Forestry Research (CIFOR), Bogor 16115, Indonesia
[c] Department of Soil Science of Temperate Ecosystems, Georg-August University Göttingen, Büsgenweg 2, Göttingen 37077, Germany
[d] Department of Agricultural Soil Science, Georg-August University Göttingen, Büsgenweg 2, Göttingen 37077, Germany
[e] Institute of Environmental Sciences, Kazan Federal University, 420049 Kazan, Russia
[f] Agro-Technological Institute, RUDN University, 117198 Moscow, Russia
[g] Center for Isotopes and Radiation Application, National Nuclear Energy Agency (BATAN), Jl. Lebak Bulus Raya No. 49, Jakarta 12440, Indonesia
[h] Department of Geophysics and Meteorology, Bogor Agricultural University, Bogor 16680, Indonesia
[i] Faculty of Agriculture, University of Papua, Manokwari 98314, Indonesia
[j] Department of Geography, National University of Singapore, 1 Arts Link, Singapore 117570, Singapore
[k] Center for International Forestry Research (CIFOR) Germany gGmbH, Bonn, Germany
[l] Plant Production, Natural Resources Institute Finland (Luke), 00790 Helsinki, Finland

ARTICLE INFO

Keywords:
Blue carbon
^{210}Pb sediment dating
Stable isotopes mixing model
Soil carbon sequestration
Climate change mitigation
Soil carbon accrual

ABSTRACT

Mangrove organic carbon is primarily stored in soils, which contain more than two-thirds of total mangrove ecosystem carbon stocks. Despite increasing recognition of the critical role of mangrove ecosystems for climate change mitigation, there is limited understanding of soil organic carbon sequestration mechanisms in undisturbed low-latitude mangroves, specifically on organic carbon burial rates and sources. This study assessed soil organic carbon burial rates, sources and stocks across an undisturbed coastal mudflat and mangrove hydrogeomorphological catena (fringe mangrove and interior mangrove) in Bintuni Bay, West Papua Province, Indonesia. ^{210}Pb radionuclide sediment dating, and mixing model of natural stable isotope signatures (δ^{13}C and δ^{15}N) and C/N ratio were used to estimate organic carbon burial rates and to quantify proportions of allochthonous (i.e., upland terrestrial forest) and autochthonous (i.e., on-site mangrove forest) organic carbon in the top 50 cm of the soil. Burial rates were in the range of 0.21–1.19 Mg C ha^{-1} yr^{-1}. Compared to the fringe mangroves, organic carbon burial rates in interior mangroves were almost twice as high. Primary productivity of C_3 upland forest vegetation and mangroves induced soil organic carbon burial in interior mangroves and this was consistent with the formation of the largest organic carbon stocks (179 ± 82 Mg C ha^{-1}). By contrast, organic carbon stored in the fringe mangrove (68 ± 11 Mg C ha^{-1}) and mudflat (62 ± 10 Mg C ha^{-1}) soils mainly originated from upland forests (allochthonous origin). These findings clearly indicate that carbon sequestered and cycling in mangrove and terrestrial forest ecosystems are closely linked, and at least a part of carbon losses (e.g., erosion) from terrestrial forests is buried in mangrove ecosystems.

1. Introduction

Mangrove forests play an important role in carbon cycling and budgets in the coastal landscape. Mangroves contribute 10–15% of global coastal carbon sequestration, despite this coastal forest only occupies 0.5% of total coastal ecosystems area – a global area of 5.3×10^9 ha composed by mangroves, seagrasses, saltmarshes, macroalgae, coral reef, unvegetated sediments, and benthic coastal ocean ecosystems (Alongi, 2014). Mangroves accumulate organic biomass annually at rates of 10.7 ± 9.4 Mg C ha^{-1} yr^{-1} *via* net primary production (NPP) (Alongi, 2014), similar to typical values for tropical evergreen and deciduous rain forests of 9.5 ± 2.6 Mg C ha^{-1} yr^{-1} (Houghton, 2003; Pregitzer and Euskirchen, 2004; Perillo et al., 2009). Despite similar NPP to other forest types, mangroves store larger amounts of total ecosystem organic carbon stocks, particularly in their organic-rich soil carbon pool. For example, total ecosystem carbon

* Corresponding author at: RIEL, Charles Darwin University, Casuarina Campus, NT 0810, Australia.
E-mail address: sigitdeni.sasmito@cdu.edu.au (S.D. Sasmito).

https://doi.org/10.1016/j.catena.2019.104414
Received 6 June 2019; Received in revised form 6 December 2019; Accepted 10 December 2019
Available online 26 December 2019

stocks stored in Indo-Pacific mangroves are up to 1023 Mg C ha^{-1} (Donato et al., 2011), which is about three to five times larger than typically found in humid lowland rainforests (cf. Jobbágy and Jackson, 2000; Pregitzer and Euskirchen, 2004; Keith et al., 2009), and similar to total ecosystem carbon stocks in tropical shallow peat swamp forests (Draper et al., 2014; Saragi-Sasmito et al., 2018). Mangrove soils are an effective carbon sink due to their capability to bury and preserve carbon within anoxic sediment conditions caused by frequent tidal inundation (Kristensen et al., 2008).

Organic carbon burial rates in mangroves typically range from 0.2 to 10.2 (mean: 2.7 ± 0.7) Mg C ha^{-1} yr^{-1} globally (Breithaupt et al., 2012; Rosentreter et al., 2018), which is about 20 times larger than terrestrial forest ecosystems (Mcleod et al., 2011). The unique tree structure and complex aerial root systems (e.g., prop roots, pneumatophores) across different mangrove species are effective at trapping organic-rich sediments (Krauss et al., 2003). Although magnitudes of particulate organic matter trapped within mangrove sediments differed depending to sediment sources (Kristensen et al., 2008), anaerobic soil condition derived from daily tidal inundation limits soil respiration and substantially facilitates more soil organic carbon preservation (Lewis 2005; Reef et al., 2010). These mechanisms are site-specific and dependent on coastal hydrogeomorphological setting, which explains the substantial variation in mangrove soil organic carbon burial rates, carbon density and carbon stocks (Woodroffe et al., 2016; Twilley et al., 2018).

Mangrove soil carbon originates from two main sources, namely allochthonous (e.g., tidally induced marine input and fluvially transported upstream sediments) and autochthonous (on-site biomass carbon input). Previous studies reported that organic matter in undisturbed mangrove soils is derived largely from autochthonous sources – identified *via* the application of carbon and nitrogen stable isotope signatures ($\delta^{13}C$ and $\delta^{15}N$; Ranjan et al., 2011; Stringer et al., 2016; Xiong et al., 2018) as well as the ratio of total organic carbon to total nitrogen contents (C/N ratio here after; Lamb et al., 2006). The $\delta^{13}C$ signature of C_3 plants including mangroves ranges from −32 to −21‰ (Bouillon et al., 2008), while C_4 plants, and marine sources such as seagrass, and algae range between −25 and −8‰ (Fourqurean et al., 1997; Lamb et al., 2006; Kennedy et al., 2010). Typical $\delta^{15}N$ signature of mangrove biomass range from 0 to 11‰ (range including outliers: −10 to 20‰, Bouillon et al., 2008; Ranjan et al., 2011), while the $\delta^{15}N$ values of seagrass and marine microalgae lie in the range of 6–12‰ and 0–4‰, respectively (Fourqurean et al., 1997; Samper-Villarreal et al., 2016). Variability of $\delta^{13}C$ and $\delta^{15}N$ values within the same vegetation tissue or end-member is commonly due to different biophysical characteristics of the study sites and anthropogenic disturbances (Bouillon et al., 2008). In addition, C/N ratio indicates vegetation nitrogen availability and uptake, and nature and intensity of organic matter diagenetic processes. For example, higher cellulose and lower protein content of vascular plants may imply a reduced availability of nitrogen due to greater C/N ratios (> 20) compared with algae (< 10; Lamb et al., 2006). Measurements of total organic carbon and nitrogen content, their ratios and stable isotope signatures from all possible end-members can be used to identify the source of buried carbon in mangrove soils. Yet, few studies have successfully combined carbon burial and source assessments in mangrove ecosystem (Serrano et al., 2018; Kusumaningtyas et al., 2019).

Here we present data on organic carbon burial rates and source patterns across coastal mudflat, fringe mangroves and interior mangroves in Bintuni Bay, West Papua Province, Indonesia. We used a ^{210}Pb sediment dating approach to quantify organic carbon burial rates (Sanders et al., 2010; Smoak et al., 2013; MacKenzie et al., 2016; Marchio et al., 2016) and a Bayesian mixing model of the combination of $\delta^{13}C$ and $\delta^{15}N$ values and C/N ratio to identify potential sources of organic carbon (Thornton and McManus, 1994; Bouillon et al., 2008; Ranjan et al., 2011; Xiong et al., 2018). Sampling locations represent a gradient of hydroperiod and geomorphological settings within an undisturbed tropical mangrove site. Soil organic carbon burial rates and physicochemical properties across sampling locations were assessed and compared. We sampled vegetation tissues as well as soils for potential end-members (mangrove foliage, mangrove non foliage, upland forest vegetation, upland forest soil), and measured their $\delta^{13}C$, $\delta^{15}N$ and C/N ratio. We first hypothesized that soil organic carbon burial rates, carbon stocks, carbon density, and carbon sources differed between sampling locations due to contrasting characteristics of vegetation composition. Second, we hypothesized that autochthonous sources are the dominant input to soil organic matter stored in mangrove locations with limited allochthonous carbon input when compared to unvegetated mudflats.

2. Materials and methods

2.1. Study site

The study was conducted in Bintuni Bay, West Papua Province, Indonesia; an area that supports more than 200,000 ha of tropical mangrove forest (Giri et al., 2011). West Papua and Papua provinces as a whole constitutes more than 10% of the world's mangrove area, and is highly diverse, with approximately 30 mangrove tree species distributed along the southwest coastline (Duke et al., 1998), and 14 species in the southern region of Bintuni Bay (Kusmana and Onrizal, 2003). Dominant species include *Sonneratia alba, Avicennia marina, Rhizophora apiculata, Rhizophora mucronata, Bruguiera parviflora,* and *Xylocarpus moluccensis*, with a maximum tree diameter of up to 80 cm and tree height up to 35 m (Sillanpää et al., 2017), representing an average biomass carbon stock of 367 ± 80 Mg C ha^{-1} (Murdiyarso et al., 2015). Over this area, mean annual precipitation is ~2750 mm, characterized by monsoonal variation with high monthly rainfall (> 250 mm) between November and April (Rouw et al., 2014). Bintuni Bay has a semi-diurnal macro-tidal cycle ranging from 3 to 6 m (Kusmana and Onrizal, 2003). Site climatic and tidal characteristics may impact the seasonal variation of sediment deposition across the study sites.

Sampling was conducted along the Tifa Creek, representative of a tide-dominated estuarine mangrove type. The distribution of sampling locations across the mudflat, fringe mangrove, and interior mangrove stands, and upland forest is shown in Fig. 1. Coastal sampling locations represent intertidal gradient, from low intertidal zone in the mudflat to higher intertidal zones in the fringe and interior mangroves, respectively. From the mudflat, fringe mangrove sampling location was located approximately 250 m, while interior mangrove was nearly 10 km. The mudflat location is nearly free of woody vegetation, while fringe and interior mangrove locations consist of mangrove forests of differing species assemblages. The fringe mangrove was dominated by a single species, *Avicennia marina,* with tree heights ranging from 5 to 10 m. By contrast, the interior mangrove was a multispecies stand with *Sonneratia alba, Avicennia marina, Rhizophora mucronata, Rhizophora apiculata, Bruguiera parviflora,* and *Xylocarpus moluccensis* present. This assemblage type is common across interior mangroves of Bintuni Bay. The distribution of mangrove forests in this bay was recently described by Sillanpää et al. (2017), who surveyed these stands and recorded a mean basal area of 29 m^2 ha^{-1} with a mean canopy height of 22 m. Surveys by Sillanpää et al. (2017) were partly conducted at undisturbed mangroves within 15 km of our site, and within a similar hydrogeomorphic setting and at similar distances from the coastline. In addition to the mudflat and mangrove assemblages, additional sampling was undertaken in undisturbed upland rainforest plots situated in an upper creek of the catchment (Fig. 1). The undisturbed rain forests in West Papua are typically composed by large trees, lianas, shrubs, and dominated by the community of *Sommeria leucophylaa-Paraltropis glabra* (Fatem and Sykora, 2013). Samples were collected to examine potential allochthonous organic carbon sources with possible end-members including rainforest foliage, root material, and soils, as these may

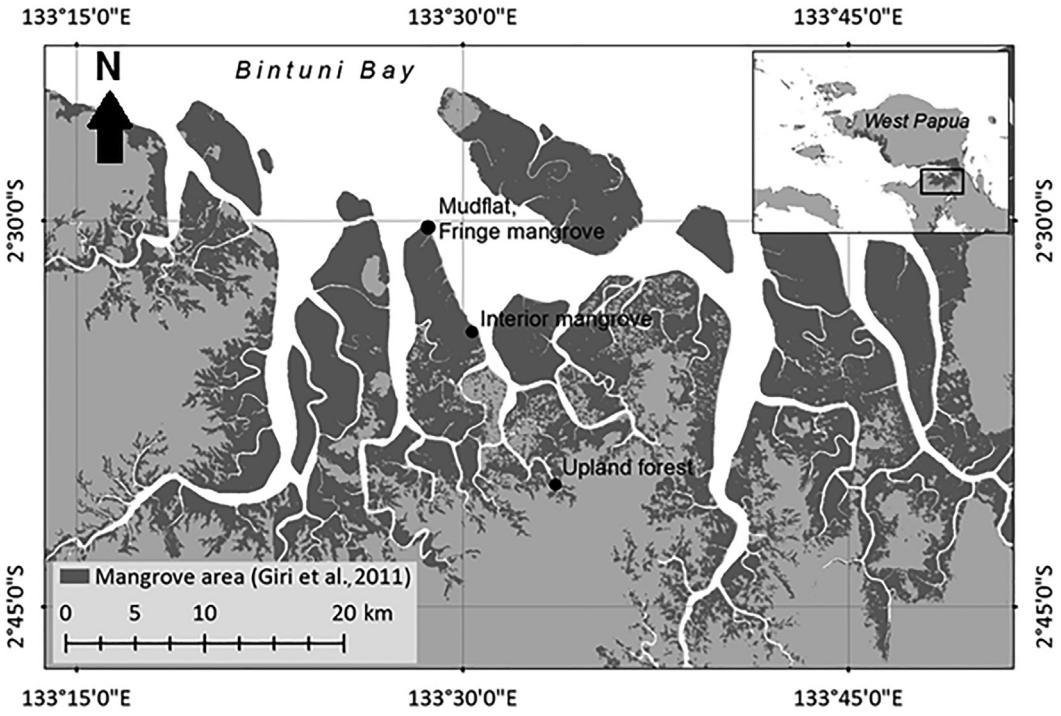

Fig. 1. Map of the study area showing mudflat, fringe mangrove forest, interior mangrove forest, and upland rainforest locations where triplicate samples were collected. These were distributed across the Tifa River catchment area at the southern part of Bintuni Bay's contiguous mangrove and upland forest area of West Papua Province, Indonesia. The map was created by using ArcMap 10.2.1 with mangrove cover data obtained from Giri et al. (2011) and land cover spatial data were freely available from Ministry of Environment and Forestry, Republic of Indonesia.

ultimately be transported to the mangrove and mudflat soils by fluvial processes. All sampling was conducted during wet season in January 2016.

2.2. Field sampling and sample preparation

Triplicate soil cores in each mudflat and mangrove locations were extracted down to 50 cm depth using an *Eijkelkamp* peat auger (Giesbeek, Netherlands). Cores were subsequently sliced into 13 sections, in which five samples of 2 cm thickness were taken from the top 10 cm section of the core, and an additional eight samples of 5 cm thickness were taken from the remaining 40 cm of the core following a standard soil sampling method for ^{210}Pb sediment dating analysis in mangroves (MacKenzie et al., 2016). Due to cost constraints, we only examined one core from each sampling location for ^{210}Pb radioisotope dating analysis using alpha spectrometry and assumed similar sediment deposition rates had occurred within the same hydrogeomorphic location. Moreover, subsampled soil cores at depths of 0–2, 4–6, 10–15, 25–30, and 45–50 cm from all triplicated sampling plots at all locations were analyzed for δ^{13}C and δ^{15}N values, total organic carbon and total nitrogen contents, and bulk density. At the upland forest location, we collected soil samples (used as end-member) from 0–5, 10–20, and 30–50 cm depth intervals from triplicated soil pits for the stable isotopes and elemental analyses only, and bulk density was not measured from here. The maximum number of replicated subsamples was taken to analyze elemental concentration and stable isotopes of carbon and nitrogen, based on the constraints of time and resources available, given the high costs for ^{210}Pb sediment dating and stable isotope analysis.

At forested sampling locations (fringe mangrove, interior mangrove, upland forest), fresh leaf, stem, root, and litter end-members were sampled. At the fringe mangrove locations, triplicate samples of fresh leaves, stems (sapwood to ~3 cm depth), root material (top 15 cm of soil), and ~50 g of leaf and twig litter were randomly sampled from the dominant species *Avicennia marina*. At the interior mangrove (from *Rhizophora mucronata*, *Rhizophora apiculata*, and *Bruguiera parviflora*) and upland forest (multiple species) locations, an identical sample regime was used. For all vegetation tissue types, δ^{13}C and δ^{15}N values, total organic carbon and nitrogen contents were analyzed. However, we only used two replicate samples of each vegetation tissue from each sampling location due to cost limitations, and assumed that elemental properties and stable isotope signatures of each tissue were not different across vegetation species (Adame et al., 2015; Werth et al., 2015).

All collected samples were dried at 40 °C until a constant weight was achieved, then samples were ground using a ball mill. For soil samples, we first removed root biomass prior to powdering step. We removed any potential inorganic carbon content from mangrove soil samples prior to elemental and stable isotope analyses by acidification (Komada et al., 2008). Following this, 5 g subsamples were rinsed with 5–10 mL of 1 M HCl and dried at 60 °C for 48 h. This procedure was repeated three times to ensure all carbonates were removed. Although rinsing procedure is commonly applied for coastal sediment organic carbon assessment (Fourqurean et al., 2014), this treatment may still release part of the soil samples, therefore stable isotope and elemental analyses results could be biased or modified (Carabel et al., 2006; Ryba and Burgess, 2002).

2.3. ^{210}Pb sediment dating

Soil accretion rates (mm yr^{-1}) were assessed using the constant rate of supply (CRS) ^{210}Pb radioisotope dating technique through alpha spectrometry analysis (Sanchez-Cabeza et al., 1999; Sanchez-Cabeza and Ruiz-Fernández, 2012; Lubis, 2013). The ^{210}Pb radioisotope is part of the ^{238}U natural decay series with a half-life of 22.2 years, thereby allowing ~150 years of sediment deposition to be dated. We followed the detailed procedure for sample preparation and analysis given by Lubis (2013) for ^{210}Pb sediment dating. About 5 g of powdered soil subsamples from all 13 layers of three cores were prepared, and ^{209}Po radioisotope tracer was added. All samples were subsequently dissolved

using HCl, HNO_3, H_2O_2, and H_2O. Iron was reduced with ascorbic acid, and ^{209}Po and ^{210}Po were deposited onto copper disks while stirring for 3 h to produce a thin film. Polonium isotopes were counted with an alpha spectrometer equipped with a passivated implanted planar silicon (PIPS) detector. ^{210}Pb was assumed to be in radioactive equilibrium with ^{210}Po in soil samples. Background information or information known about supported ^{210}Pb activity (in equilibrium with ^{226}Ra in soils) was obtained from the constant activity of the deepest samples in cores measured by alpha spectrometry (*sensu* de Carvalho et al., 2011; Cossa et al., 2014). Residual excess (unsupported) of ^{210}Pb activity was obtained from the subtraction of supported ^{210}Pb activity from total ^{210}Pb activity (Appleby, 1998; Lubis, 2013), and used as one of variables to calculate the time of sediment deposition at each layer. Both supported and unsupported ^{210}Pb activities were measured in Becquerels per kilogram (Bq kg^{-1}). Sediment or soil mass accumulation rate (g cm^{-2} yr^{-1}) was the product of sediment dry weight (g) per core area (cm^2) and time of sediment deposition (yr). Moreover, sediment accretion rates (mm yr^{-1}) were obtained by multiplying soil mass accumulation rate and bulk density (g cm^{-3}). The use of CRS model and alpha spectrometry analysis may have some limitations (e.g., low efficiency of sample requirement for the analysis, coarse accuracy of detection limit, and time constraint, MacKenzie et al., 2016). All of these limitations may contributed to the uncertainty of this study findings, however, we had limited resources to overcome and improve these approaches (e.g., direct unsupported ^{210}Pb detection by using gamma spectrometry and rapid steady-state mixing (RSSM) model for calculating sediment accretion rates, *sensu* MacKenzie et al., 2016; Soper et al., 2019). Detailed results of ^{210}Pb sediment dating and calculation of soil accretion rates are provided in CIFOR Dataverse digital repository system (Sasmito et al., 2019).

2.4. Stable isotope and elemental analyses

Selected soil and vegetation tissue samples were analyzed for carbon and nitrogen stable isotope ($\delta^{13}C$ and $\delta^{15}N$). Isotopic ratios are presented using conventional delta (δ) nomenclature and were calculated from the following equation: δ (‰) = $((R_{sample}/R_{standard}) - 1) \times 1{,}000$, where R_{sample} is either the stable $^{13}C/^{12}C$ or $^{15}N/^{14}N$ isotope ratio, and $R_{standard}$ is the isotopic signature value of the standardized international Vienna-Pee Dee Belemnite (V-PDB) for $\delta^{13}C$ and atmospheric N_2 for $\delta^{15}N$. The $\delta^{13}C$ and $\delta^{15}N$ signatures were analyzed using isotopic-ratio mass spectrometry (IRMS) (Delta Plus; Finnigan MAT, Bremen, Germany), while elemental organic carbon and nitrogen analyses were performed using an NA1110 analyzer (CE Instruments, Milan, Italy). The C/N ratio was the ratio between total organic carbon and nitrogen contents.

2.5. Organic soil carbon burial and stock calculation

Bulk density in mudflat and mangrove soils was obtained from the ratio between dry mass (g) and sample volume (cm^{-3}) determined from the auger dimensions and sample thickness (cm). Organic carbon (OC) burial rates (Mg C ha^{-1} yr^{-1}) were calculated using Equation (1):

$$\text{Soil } OC_{burial} = BD \times C_{org} \times SAR \quad (1)$$

where BD is soil bulk density (g cm^{-3}), C_{org} is total organic carbon content (%), and SAR is soil accretion rates (mm yr^{-1}) derived from ^{210}Pb sediment dating. Soil organic carbon stocks (OC_{stock}) (Mg C ha^{-1}) were calculated using Equation (2):

$$\text{Soil } OC_{stock} = BD \times C_{org} \times H \quad (2)$$

where BD is soil bulk density (g cm^{-3}), C_{org} is total organic carbon content (%), and H is soil layer thickness (cm). Although soil samples used for stable isotope and elemental analyses were root-free, bulk density estimates for fringe and interior mangroves may be underestimated due to extensive fine root biomass volume. Therefore, calculated soil carbon burial and stocks from these locations could possibly underestimate.

2.6. Organic carbon source and mixing model

Soil organic carbon sources and their relative contributions were assessed using a stable isotope mixing model. The mixing model was run using a Bayesian stable isotope mixing model *via* the R Statistic SIMMR package which widely applied for food-web studies (Parnell et al., 2010; Parnell and Inger, 2016). Compared with a simple two-end mixing model (Bouillon et al., 2008), SIMMR has been recently used in stable isotope for ecological studies because of its ability to use multiple end-members, isotopes and other physicochemical properties (e.g., C/N ratio). In addition, the Markov Chain Monte Carlo function within SIMMR provides detailed uncertainties of end-members' relative contribution (Samper-Villarreal et al., 2016; Mabit et al., 2018; Serrano et al., 2018; Kusumaningtyas et al., 2019). The detailed information of data and statistical procedures for this SIMMR mixing model are described by Parnell and Inger (2016).

We first defined *a priori* model variable inputs ($\delta^{13}C$ and $\delta^{15}N$ values, and C/N ratio) and 15 potential end-members (vegetation leaf, stem, root, litter respectively from fringe mangrove, interior mangrove and upland forest, as well as upland forest soil, marine algae, and seagrass). All stable isotopic signatures and C/N ratios were obtained from the field as described above, except for additional values for marine algae and seagrass end-members, which were obtained from the literature (Chen et al., 2017; Fourqurean et al., 1997; Kennedy et al., 2010; Lamb et al., 2006; Samper-Villarreal et al., 2016; Wahyudi and Afdal, 2019). We compared $\delta^{13}C$ and $\delta^{15}N$ values, and C/N ratio between collected end-members samples and between collected soil samples from mudflat, fringe mangrove and interior mangrove locations (see summary of statistical analysis in Table 1). Additional values of $\delta^{13}C$ and $\delta^{15}N$, and C/N ratios were obtained from literature which report datasets collected from coastal ecosystems across Indonesia. To

Table 1
Total organic carbon and nitrogen contents, C/N ratio, and $\delta^{13}C$ and $\delta^{15}N$ signatures in biomass in mangrove and upland forests. Letters in the end of physicochemical properties value denote significant difference of physicochemical properties value ($p < 0.05$) among tissue types.

Location	Vegetation tissue	Total organic carbon content (%)	Total nitrogen content (%)	C/N ratio	$\delta^{13}C$ (‰)	$\delta^{15}N$ (‰)
Mangrove	Leaf	43.52 ± 0.40 (4)^{a}	1.41 ± 0.21 (4)^{a}	33.57 ± 6.29 (4)^{a}	−31.7 ± 0.5^{a}	2.7 ± 0.6^{a}
	Litter	41.25 ± 1.29 (4)^{ab}	0.60 ± 0.02 (4)^{b}	69.10 ± 1.05 (4)^{a}	−30.5 ± 0.3^{ab}	2.5 ± 0.6^{a}
	Root	39.33 ± 0.90 (4)^{b}	0.47 ± 0.07 (4)^{b}	91.69 ± 16.81 (4)^{a}	−29.7 ± 0.6^{ab}	3.0 ± 0.6^{a}
	Stem	46.06 ± 0.33 (4)^{ac}	0.16 ± 0.01 (4)^{b}	298 ± 22 (4)^{c}	−29.4 ± 0.4^{b}	2.0 ± 0.1^{a}
Grand mean		42.54 ± 0.75 (16)	0.66 ± 0.13 (16)	123 ± 27 (16)	−30.3 ± 0.3	2.5 ± 0.3
Upland forest	Leaf	47.09 ± 1.66 (2)^{a}	1.90 ± 0.53 (2)^{a}	27.17 ± 8.46 (2)^{a}	−32.9 ± 0.8^{a}	0.2 ± 1.4^{a}
	Litter	45.92 ± 2.97 (2)^{a}	1.16 ± 0.01 (2)^{a}	39.56 ± 2.96 (2)^{a}	−30.9 ± 1.3^{a}	−0.2 ± 0.04^{a}
	Root	45.57 ± 0.19 (2)^{a}	0.99 ± 0.04 (2)^{a}	46.02 ± 1.56 (2)^{a}	−31.3 ± 1.3^{a}	−1.4 ± 0.2^{a}
	Stem	48.07 ± 0.51 (2)^{a}	0.28 ± 0.02 (2)^{a}	174 ± 13 (2)^{b}	−31.1 ± 0.2^{a}	2.1 ± 1.3^{a}
Grand mean		46.66 ± 0.75 (8)	1.08 ± 0.24 (8)	71.81 ± 22.75 (8)	−31.5 ± 0.5	0.2 ± 0.6

Note: All data are presented as the mean ± standard error of the mean.

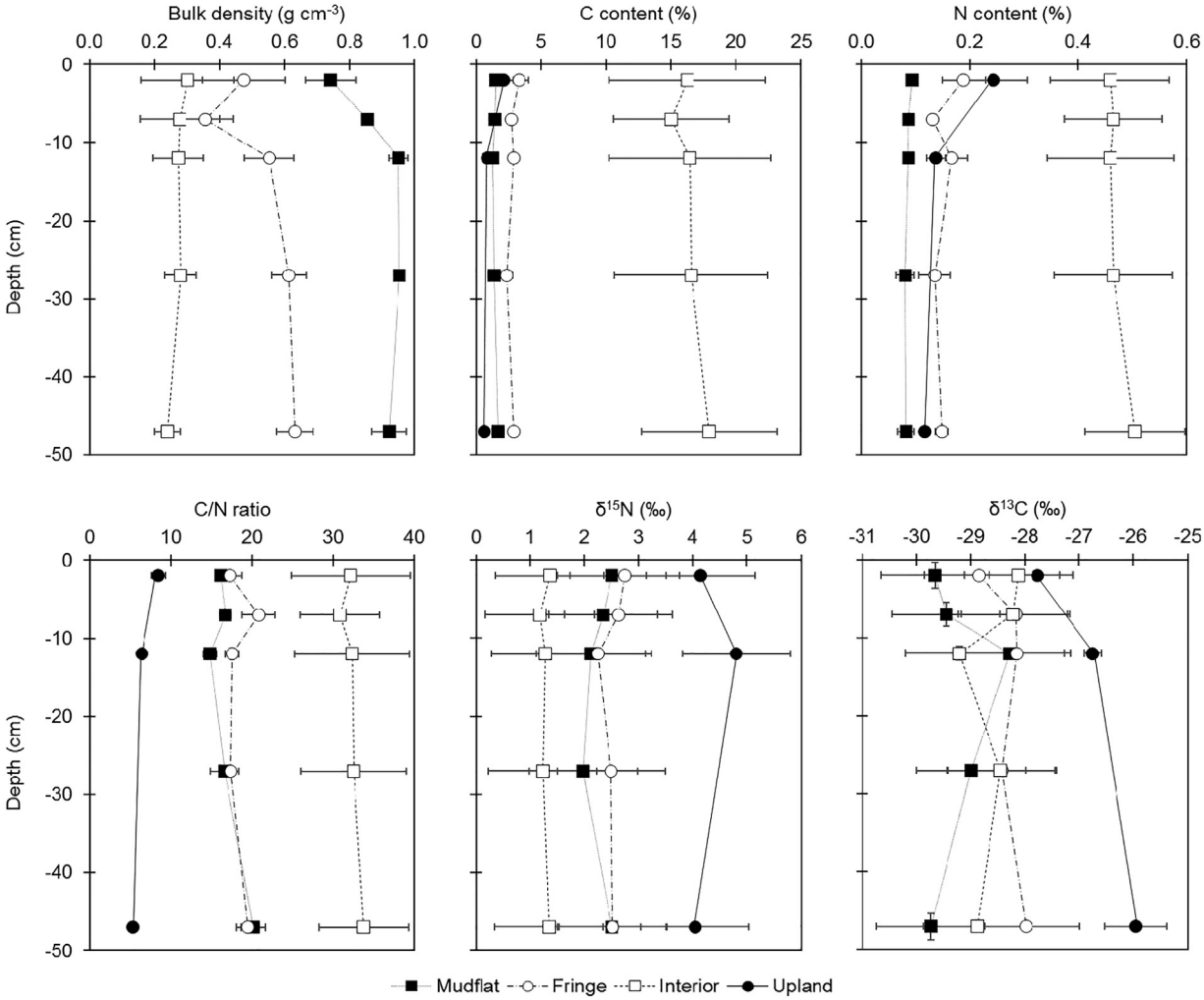

Fig. 2. Soil bulk density, total organic carbon content, total organic nitrogen content, C/N ratio, $\delta^{15}N$, and $\delta^{13}C$ values in mudflat, fringe mangrove, interior mangrove, and upland forest down to a soil depth of 50 cm. Error bars indicate standard error of the mean across triplicated plots for each sampling location (n = 3).

simplify results interpretation of the mixing model output and due to low sample size of some end-members, we grouped sources proportion as suggested by Phillips et al. (2014). We combined source proportion of vegetation foliage, litter, root and stem end-members from fringe mangrove and interior mangroves into all mangrove vegetation tissues, and vegetation foliage, litter, root and stem end-members from upland forest into all upland forest vegetation tissues, as well as marine algae and seagrass end-members into marine algae + seagrass. This output combination gave a four organic carbon sources of mixing model proportion results that consisted of (1) all mangrove vegetation tissues, (2) all upland forest vegetation tissues, (3) upland soil, and (4) marine algae + seagrass driven using three input variables, (1) $\delta^{13}C$ values, (2) $\delta^{15}N$ values and (3) C/N ratio.

The SIMMR mixing model was run three times by using three different input variable combinations, (1) $\delta^{13}C$ and $\delta^{15}N$ values, (2) $\delta^{13}C$ values and C/N ratio, and (3) $\delta^{13}C$ and $\delta^{15}N$ values and C/N ratio (see Supplementary Information 1 for detailed results of the all mixing model). Three different combinations were applied to minimize error of output proportion results that sourced by input variables. The final source proportions were the mean product of these three mixing model applications with their final standard deviation was calculated following error propagation rule.

2.7. Statistical analysis

Significant differences of physicochemical properties between soil and vegetation variables, sampling locations and soil depths were assessed using analysis of variance (ANOVA) and pairwise comparison with Bonferroni *p*-value adjustment method. All data normality distributions were examined using the Shapiro–Wilk test of normality, and a logarithmic normal data transformation was applied, particularly for soil organic carbon and C/N ratio prior to ANOVA. All statistical analyses were performed using R Statistic software version 3.5.0 (R Core Team, 2018). ANOVA results are summarized in Supplementary Information 2, while multiple comparison results are provided in Supplementary Information 3. All data produced and used by this work are available through CIFOR Dataverse digital repository system (Sasmito et al., 2019).

3. Results

3.1. Physicochemical properties of soil and vegetation

The mean values of soil bulk density, total organic carbon, total nitrogen, and C/N ratio were significantly different across locations ($p < 0.001$, Fig. 2), except for total organic carbon and C/N ratio were similar between mudflat and fringe mangrove (see multiple comparison results in Supplementary Information 3). Interior mangrove soils had the highest mean values (± SD) of total organic carbon content (16.4 ± 2.1%), total nitrogen content (0.47 ± 0.04%), and C/N ratio (32.3 ± 2.4). Soil bulk density was greatest in mudflats (0.9 ± 0.1 g cm^{-3}) and lowest in interior mangrove soils

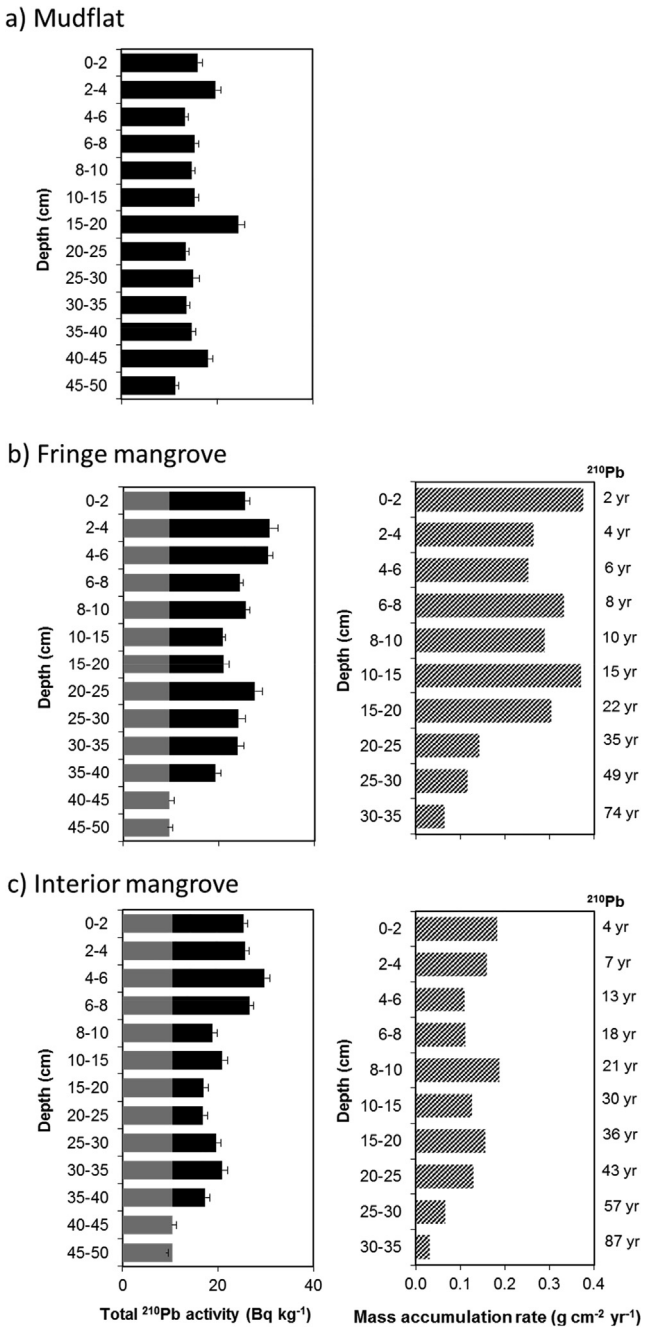

Fig. 3. Total ^{210}Pb activity, soil mass accumulation rates, and ages of (a) mudflat, (b) fringe mangroves, and (c) interior mangroves. Grey bars of first column figures denote supported ^{210}Pb activity, while dark-colored bars denote unsupported ^{210}Pb activity. Note: X-axis scale and title of panels A and B follow panel C.

(0.3 ± 0.1 g cm^{-3}), while the soil bulk density of fringe mangrove soils was intermediate (0.5 ± 0.2 g cm^{-3}). Pooled means of C/N ratios for mudflat and mangrove soils were 22.6 ± 8.9, significantly higher than for mineral soils of the upland forests (6.8 ± 1.6). The means of total organic carbon and nitrogen contents differed across vegetation tissues within mangrove locations ($p < 0.001$), except for the total nitrogen contents of litter, root, and stem were similar (Table 1, Supplementary Information 2). However, total organic carbon and nitrogen contents were similar among the upland forest vegetation tissues. The C/N ratios across vegetation tissues within both mangrove and upland forests were statistically different ($p < 0.05$), except for leaf, litter and root tissues were similar (Table 1, Supplementary Information 2).

3.2. ^{210}Pb activities and carbon burial rates

The unsupported ^{210}Pb activities in fringe mangrove and interior mangrove soil cores decreased with depth (Fig. 3). However, we did not find similar trend in mudflat location which may be due to rapid physical and biological perturbation that resulted in substantial sediment mixing; thus soil accumulation rates could not be calculated at this location. Mean soil mass accumulation rates were greater in fringe mangroves (0.25 ± 0.10 g cm^{-2} yr^{-1}) compared to interior mangroves (0.13 ± 0.07 g cm^{-2} yr^{-1}) (Fig. 3, Table 1). Expressed as a depth change per year, these rates equate to 3.9 ± 0.7 and 2.5 ± 0.3 mm yr^{-1} of soil accretion rates for fringe and interior mangroves, respectively (Fig. 4). Overall, the top 50 cm soil of fringe and interior mangroves was deposited during the last 74 and 87 years, respectively

Organic carbon densities, carbon burial rates, and carbon stocks differed across mangrove locations, but, except organic carbon stocks, they were unaffected by soil depth ($p < 0.05$, Fig. 4). The largest mean organic carbon density, carbon burial rates, and carbon stock values were all found at the interior mangrove location, with 3.7 ± 1.7 g C cm^{-3}, 0.9 ± 0.4 Mg C ha^{-1} yr^{-1}, and 179 ± 82 Mg C ha^{-1}, respectively (Fig. 4). At the fringe mangrove location, organic carbon burial rates were half the value of those at the interior mangrove location (0.5 ± 0.2 Mg C ha^{-1} yr^{-1}). Organic carbon density and carbon stocks at the fringe mangrove (1.4 ± 0.4 g C cm^{-3} and 68 ± 11 Mg C ha^{-1}) and mudflat (1.3 ± 0.5 g C cm^{-3} and 62 ± 10 Mg C ha^{-1}) areas were similar ($p > 0.05$).

3.3. Stable carbon ($\delta^{13}C$) and nitrogen ($\delta^{15}N$) isotope signatures

The mean of the soil δ^{13}C signatures was similar between mudflat, fringe mangrove and interior mangrove locations, while the δ^{15}N signatures were statistically different ($p < 0.001$, Fig. 2, Supplementary Information 2). The means of soil δ^{15}N signatures were 2.3 ± 0.4, 2.5 ± 0.3, and 1.7 ± 0.7‰ at mudflat, fringe mangrove, and interior mangroves, respectively. Across mangrove tissues, δ^{13}C signatures were statistically different and an increasing pattern was observed from leaves (−31.7 ± 1.0‰) to stems (−29.4 ± 0.7‰) ($p < 0.05$, Table 1, Fig. 5, Supplementary Information 2); the δ^{15}N signatures, in contrast, were similar for all tissues (Table 1, Fig. 5, Supplementary Information 2). In the upland forest vegetation tissues, both δ^{13}C and δ^{15}N signatures were similar ($p > 0.05$, Table 1). Both δ^{13}C and δ^{15}N signatures were similar toward 50 cm of soil depth across all sampling locations (Fig. 2).

3.4. Source of deposited soil organic matter

Soil organic carbon sources across mudflat, fringe mangroves and interior mangroves were dominated by organic carbon sources originating from mangrove tissues (autochthonous source) and upland forest vegetation tissues, as well as upland forest soil (allochthonous source) (Fig. 6). The dominant source of organic carbon stored in mudflats and fringe mangroves were allochthonous upland forest soils (Fig. 6). We observed a high contribution (56.9 ± 11.4%) of allochthonous upland forest vegetation in interior mangrove soils. From seaward (mudflat) to landward (interior mangrove), the proportion of soil organic carbon originating from allochthonous upland forest soils (through sedimentation) decreased from 56.4 ± 5.5% to 12.3 ± 10.5%, while organic carbon originating from autochthonous mangrove tissues increased from 4.8 ± 1.7% to 23.5 ± 12.7% (Fig. 6).

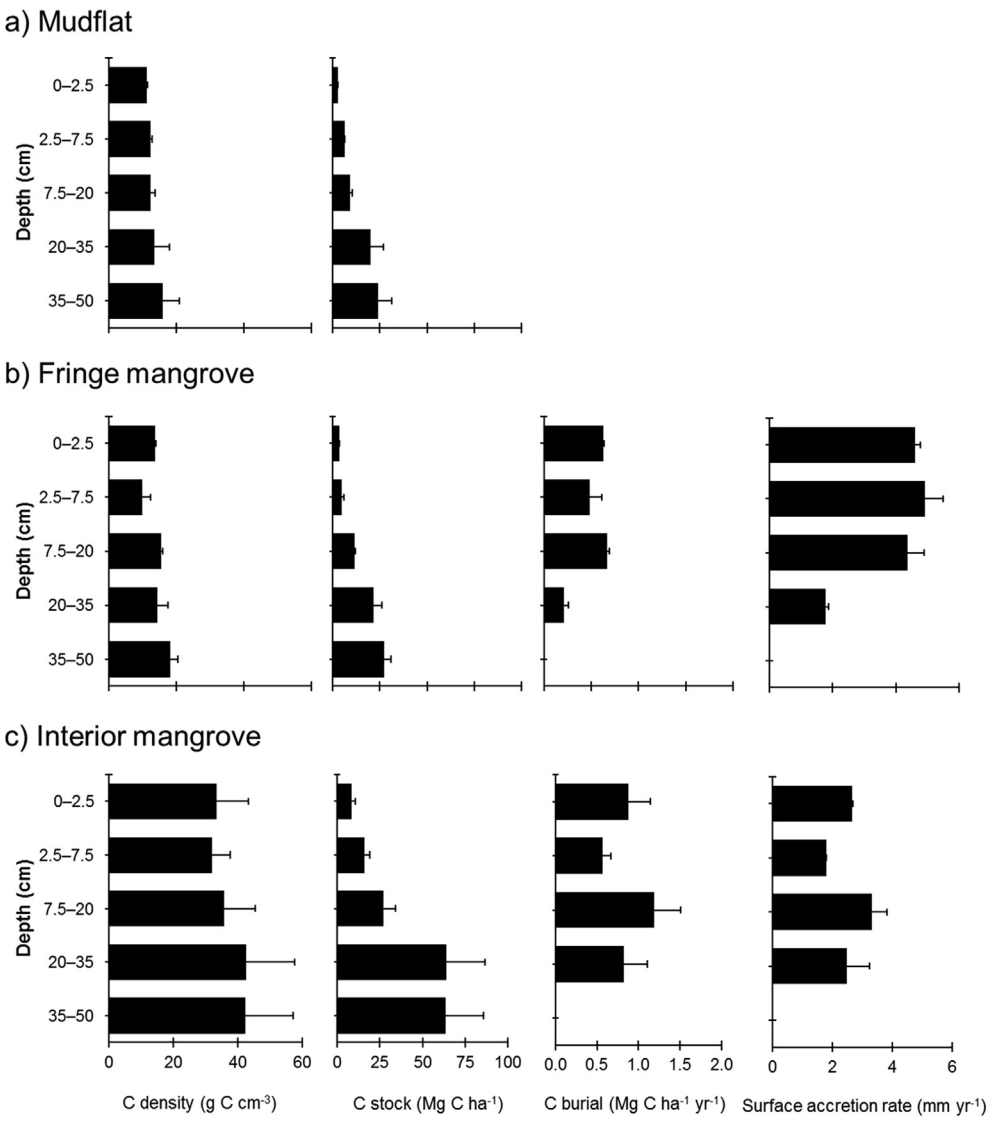

Fig. 4. Organic carbon density, carbon stock, and carbon burial and surface accretion rates across mangrove locations, (a) mudflat, (b) fringe mangrove, and (c) interior mangrove (mean ± SE). Organic carbon burial and surface accretion rates in the mudflat location could not be determined due to sediment mixing.

4. Discussion

4.1. Burial rates and source of organic carbon in mangrove soils

The examined coastal mudflat and mangrove ecosystems revealed the existence of concomitant mechanisms explaining variation in patterns of soil carbon burial, density, stocks and source, and in agreement with our first hypothesis. It is apparent that soil properties, vegetation density, and inferred productivity are closely coupled across study sites, with geomorphic setting, hydroperiod, and stand characteristics determining soil total organic carbon and nitrogen contents, organic carbon burial rates, and ultimately soil organic carbon storage as shown in Fig. 7. Mudflat and fringe mangroves had similar organic carbon densities and stocks, despite the presence of aboveground stands in the fringe mangrove (Fig. 7). It is presumably due to the reason that fringe mangrove soils used to be mudflat as we observed seedlings establishment or mangrove encroachment onto the mudflat area. Contrastingly, organic carbon density and stock in soils of interior zone were three times larger than in fringe mangrove and mudflat, most likely due to substantial organic carbon inputs produced by the combination of vegetation tissues from mature upland forest and mangrove (Fig. 6) – i.e., net primary productivity (NPP). Despite the age of buried sediments in the fringe and interior mangroves zones being similar (Fig. 3), surface accretion rates in fringe mangroves (i.e., input of sediments containing allochthonous organic carbon) was almost twice than of interior mangroves (Fig. 4b). This suggests that organic carbon stocks and sources of stored organic carbon depend on both i) forest structure and NPP of mature mangrove forests and ii) accretion rates of allochthonous organic carbon-containing sediments.

Organic carbon burial rates observed in this study ranged between 0.21 and 1.19 Mg C ha^{-1} yr^{-1}, with higher burial rates in interior mangroves compared to fringe mangroves, similar to previous findings in Florida mangroves (Marchio et al., 2016). Interior mangroves are likely to have an optimal hydroperiod for mangrove stand growth (Krauss et al., 2006, 2007; Crase et al., 2013), with lower wave energy and tidal inundation, while inflow of nutrient-rich fresh water from upstream systems promoting tree growth (i.e., NPP; Krauss et al., 2007). This is consistent with results of studies assessing plant productivity (e.g., basal area, total volume, litter fall) of mangroves in Bintuni Bay (Sillanpää et al., 2017) and a similar mangrove forest ecosystem in Borneo (Sukardjo et al., 2013). The reduction of hydrological flushing in interior mangroves additionally supports the accumulation of organic carbon-rich benthic and litter mats on the soil surface (McKee, 2011; Krauss et al., 2014) and subsequent

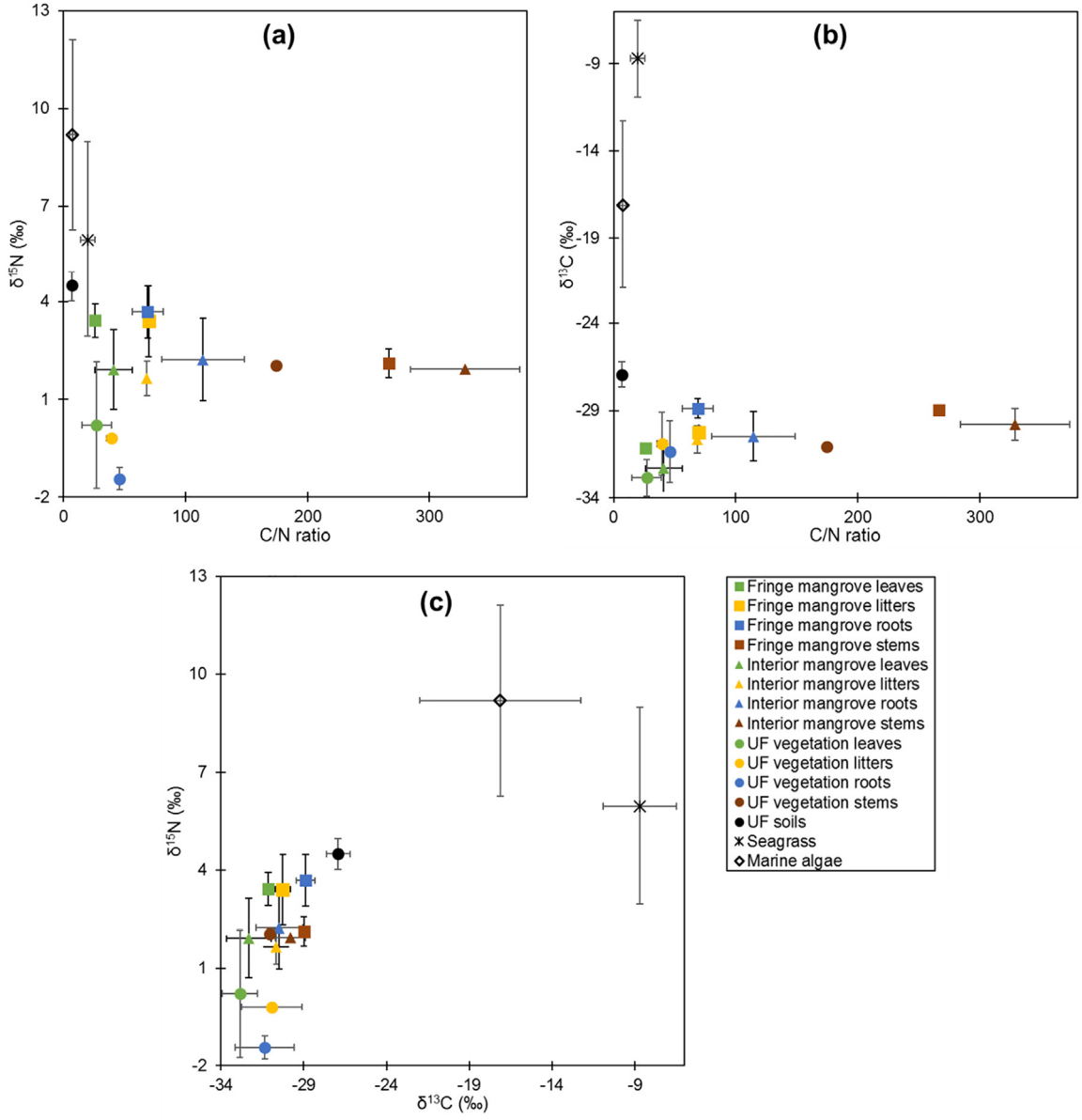

Fig. 5. Summary mean and standard deviation of (a) C/N ratio vs $\delta^{15}N$, (b) C/N ratio vs $\delta^{13}C$, (c) $\delta^{13}C$ vs $\delta^{15}N$ values, and across collected samples with additional data on marine algae from Lamb et al. (2006) and Samper-Villarreal et al. (2016), and on seagrass from Fourqurean et al. (1997) and Wahyudi and Afdal (2019). Note: UF = upland forest.

decomposition and bioturbation into the top layer of the soil column (Kristensen, 2008; Robertson, 1991). Detecting sediment profile age of mixed sediments using ^{210}Pb is limited, as we observed in the mudflat site where it can be caused by the presence of intense perturbations (Ranjan et al., 2011; Smoak et al., 2013). The present of vegetation in fringe and interior mangroves could further support sediments stabilization, hence total ^{210}Pb activity pattern over soil cores (Fig. 3b-c) were relatively consistent with deepest soil cores had lowest total ^{210}Pb activity – assigned as supported ^{210}Pb activity. By contrast, we observed unclear pattern of total ^{210}Pb activity of mudflat soil core, which may be due to less stabilized sediments resulted from biophysical perturbations effect (e.g., erosion, deposition, pedoturbation), thus supported ^{210}Pb activity was undetected.

Although mangrove forests promote stabilization of sediments and production of biomass carbon in fringe and interior zones, carbon burial rates in the top 50 cm of soil (0.68 ± 0.39 Mg C ha^{-1} yr^{-1}) was three times lower than global carbon burial rates (Breithaupt et al., 2012; Rosentreter et al., 2018). This is presumably due to low surface accretion rates (3.1 ± 1.3 mm yr^{-1}), which is slightly lower than global average of surface accretion rate in undisturbed conserved mangrove (3.6 ± 0.4 mm yr^{-1}; Pérez et al., 2018). Low accretion rates, however, indicate presence of intact upland forests that have low levels of soil erosion (Labrière et al., 2015) compared to large sediment accretion rates of 10.5 mm yr^{-1} assessed in the Ajkwa River area – approximately 500 km to southwest from Bintuni Bay – where hinterland deforestation and mining activities were induced (Brunskill et al., 2004). Therefore, the input of allochthonous sediments may differ between locations and affect organic carbon burial and source in mangrove soils substantially.

We observed a larger contribution of allochthonous sources compared to autochthonous sources across mudflat and mangrove soils, which is unlike what we expected in the second hypothesis. The relative proportion of allochthonous and autochthonous organic carbon sources across the mudflat-mangrove assemblage was gradational (Fig. 7). Given higher contribution of upland forest soils source at seaward compares to landward coastal positions, fluvial transport within the

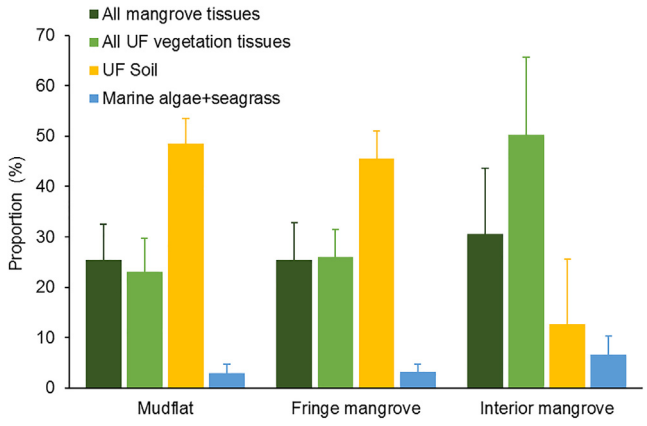

Fig. 6. Relative contribution of sources to soil organic matter across (a) mudflat, (b) fringe and (c) interior mangroves in Bintuni Bay. Left panel shows the source histograms on the diagonal, contour plots and correlation between the sources on the upper and lower diagonals, respectively. Large negative correlations indicate that the mixing model cannot distinguish between the two sources, while large positive correlations indicate that two sources contribute to soil organic matter substantially and distinctively. Right panel shows the quantile boxplot of the sources contribution to soil organic matter. Note: UF = upland forest.

catchment plays a key role in transferring eroded organic material from terrestrial upland forests into the coastal area. These transported sediments first enter to the lower elevation at mudflat area rather than higher elevation at landward forest (Sanders et al., 2010). Autochthonous organic carbon from mangrove trees stored in interior mangrove soils was associated with significantly lower $\delta^{15}N$ signature and higher C/N ratios (see Fig. 2), and older mix species forest stands compared to younger mono specific fringe mangrove.

The $\delta^{13}C$ and $\delta^{15}N$ signatures were not significantly different across the top 50 cm of the soil profile in each mudflat, fringe and interior mangroves, which is similar to previous studies conducted in estuarine mangroves of Borneo and Central Java (Weiss et al., 2016; Kusumaningtyas et al., 2019). Lacking variation of $\delta^{13}C$ and $\delta^{15}N$ signatures in mangrove soils up to a depth of 50 cm indicated limited microbial decomposition of soil organic carbon as a function of the anoxic soil environment. Compared to other studies with dominant soil organic carbon source from seagrass tissue observed in the Northern Sulawesi (Chen et al., 2017) and Western Indonesia (Wahyudi and Afdal, 2019), the mean of soil $\delta^{13}C$ from our study site is relatively low (more depleted in ^{13}C), suggesting dominant contribution of C_3 mangrove and upland forest sources. While limited, $\delta^{13}C$ assessment conducted in coastal ecosystems of Indonesia (Supplementary Information 4) suggest that $\delta^{13}C$ values from mangrove tissues in our study were within the range of mangrove species-specific $\delta^{13}C$ values obtained from estuarine and riverine mangroves (Weiss et al., 2016). We observed that current studies on organic carbon source as well as organic carbon burial in Indonesia are limited by low number of sample replication (see Supplementary Information Table 4), and thus we suggest that future similar studies should consider a larger number of samples. From this study, it is also noted that the mixing model of bulk carbon and nitrogen stable isotopes has limitations discerning the contribution between mangrove and upland forest tissues (see a high negative correlation in Fig. 6c). This limitation may be overcome by combining stable isotope with other potential semi-quantitative approaches such as compound-specific isotopes and environmental DNA (Geraldi et al., 2019).

4.2. Blue carbon and policy implications

There is a growing understanding of carbon storage in coastal mangroves – together with seagrasses and saltmarshes – as "blue carbon" ecosystems. These carbon-rich ecosystems could contribute to offsetting greenhouse gas emissions to the atmosphere by avoiding their loss (Duarte et al., 2013; Murdiyarso et al., 2015; Howard et al., 2017). This study furthers our understanding of the source of the vast soil carbon sequestration capacity available from undisturbed tropical tide-dominated mangroves in West Papua, where such of data are limited. This study suggests the important role of mangrove forests in maintaining a significant coastal soil carbon pool (*via* autochthonous carbon production) and trapping organic-rich sediment from within the catchment area. This demonstrates the connectivity between coastal

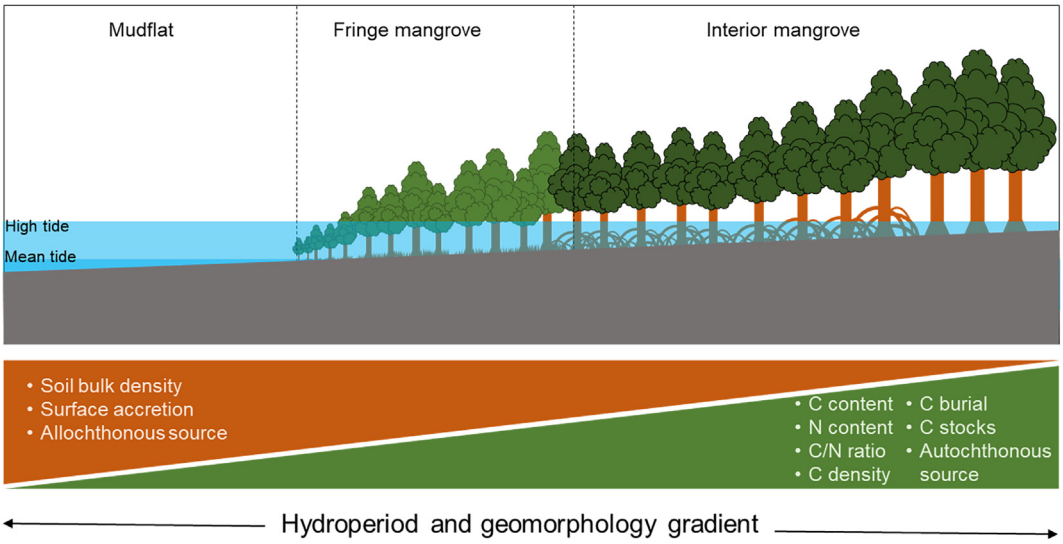

Fig. 7. A conceptual diagram summarizing organic carbon burial and source pattern resulting from the variations of biological and physical factors across hydroperiod and geomorphological gradients of near-pristine tidal-dominated estuarine mangroves in Bintuni Bay, West Papua Province, Indonesia. Top panel illustrates the condition of sampling locations where we observed typical biological (forest structure and composition) and physical (hydroperiod and tidal inundation) factors differ across mudflat, fringe, and interior mangroves. Bottom panel describes patterns of soil organic carbon dynamic and other physicochemical properties obtained from the top 50 cm depth from this study. Brown triangle shows the decrease of soil bulk density, surface accretion, and allochthonous sediments from mudflat (seaward) to interior mangrove (landward). By contrast, green triangle represents the increase of soil total organic carbon content, soil total nitrogen content, C/N ratio, organic carbon density, organic carbon burial, organic carbon stocks, and autochthonous contribution.

and inland terrestrial forests in maintaining coastal carbon. Connectivity explains spatial patterns of carbon burial rates, carbon sources, and ultimately carbon storage in mangroves and mudflats. Future scaled-up studies on blue carbon should consider variation in hydrogeomorphological setting and the need for high spatial replication to reduce uncertainty.

Mangrove forests in Indonesia represent 26–29% of the global mangrove forest, with ongoing losses due to deforestation (Hamilton and Casey, 2016). To manage and conserve mangrove carbon stocks, consideration needs to be given to inland habitats as well as adjacent marine ecosystems and their conservation status at the catchment scale. The Government of Indonesia has proposed a 29% greenhouse gas emissions reduction by 2030, with a major contribution (60%) expected from the forestry sector, which under current Indonesian policy settings includes mangrove forests (Government of Indonesia, 2016). There are increasing threats from development and natural utilization in both marine and upland landscapes in the West Papua region (Ginting and Pye, 2013; Andrianto et al., 2014), particularly from mining and mangrove forest conversion to oil palm plantations (Richards and Friess, 2016). Widespread conversion of mangrove stands such as those examined in this study could result in a significant loss of captured carbon. Carbon would likely be lost to near-shore waters, thereby degrading water quality and increasing coastal emissions, an outcome contrary to the national goals of improved land management that contributes to reductions in emissions.

Declaration of Competing Interest

The authors declare that they have no known competing financial interests or personal relationships that could have appeared to influence the work reported in this paper.

Acknowledgements

We thank USAID for funding support (AID-BFS-G-11-00002) to CIFOR-SWAMP. We acknowledge PT. BUMWI for field facilities assistance, KOSI-University of Göttingen and BATAN for laboratory facilities, Environmental Research Unit of West Papua Province, and KESBANGPOL, Ministry of Home Affairs, Republic of Indonesia for research permits. We thank Damien Maher who provided comments on an earlier draft of this manuscript. SDS acknowledges receipt of an Australian Government Research Training Program scholarship. NB was supported by CIM, GIZ, and the German Federal Employment Agency. YK was supported by the Government Program of Competitive Growth of Kazan Federal University and the "RUDN University program 5–100". We thank the anonymous reviewers of this manuscript for their constructive comments

Appendix A. Supplementary material

Supplementary data to this article can be found online at https://doi.org/10.1016/j.catena.2019.104414.

References

Adame, M.F., Fry, B., Gamboa, J.N., Herrera-Silveira, J.A., 2015. Nutrient subsidies delivered by seabirds to mangrove islands. Mar. Ecol. Prog. Ser. 525, 15–24. https://doi.org/10.3354/meps11197.

Alongi, D.M., 2014. Carbon cycling and storage in mangrove forests. Ann. Rev. Mar. Sci. 6, 195–219. https://doi.org/10.1146/annurev-marine-010213-135020.

Andrianto, A., Sedik, B.F., Waridjo, H., Komarudin, H., Obidzinski, K., 2014. The impacts of oil palm plantations on forests and people in Papua: A case study from Boven Digoel District: CIFOR Working Paper No. 163. Bogor, Indonesia: CIFOR.

Appleby, P., 1998. Dating recent sediments by 210 Pb: Problems and solutions. In: Proceedings of a Seminar, Helsinki, 2–3 April, 1997. STUK-A 145. pp. 7–24.

Bouillon, S., Connolly, R.M., Lee, S.Y., 2008. Organic matter exchange and cycling in mangrove ecosystems: Recent insights from stable isotope studies. J. Sea Res. 59, 44–58. https://doi.org/10.1016/j.seares.2007.05.001.

Breithaupt, J.L., Smoak, J.M., Smith, T.J., Sanders, C.J., Hoare, A., 2012. Organic carbon burial rates in mangrove sediments: strengthening the global budget. Global Biogeochem. Cycles 26. https://doi.org/10.1029/2012gb004375.

Brunskill, G.J., Zagorskis, I., Pfitzner, J., Ellison, J., 2004. Sediment and trace element depositional history from the Ajkwa River estuarine mangroves of Irian Jaya (West Papua), Indonesia. Cont. Shelf Res. 24, 2535–2551. https://doi.org/10.1016/j.csr.2004.07.024.

Carabel, S., Godínez-Domínguez, E., Verísimo, P., Fernández, L., Freire, J., 2006. An assessment of sample processing methods for stable isotope analyses of marine food webs. J. Exp. Mar. Biol. Ecol. 336 (2), 254–261.

Chen, G., Azkab, M.H., Chmura, G.L., Chen, S., Sastrosuwondo, P., Ma, Z., Dharmawan, I.W., Yin, W., Chen, B., 2017. Mangroves as a major source of soil carbon storage in adjacent seagrass meadows. Sci. Rep. 7, 42406. https://doi.org/10.1038/srep42406.

Cossa, D., Buscail, R., Puig, P., Chiffoleau, J.-F., Radakovitch, O., Jeanty, G., Heussner, S., 2014. Origin and accumulation of trace elements in sediments of the northwestern Mediterranean margin. Chem. Geol. 380, 61–73. https://doi.org/10.1016/j.chemgeo.2014.04.015.

Crase, B., Liedloff, A., Vesk, P.A., Burgman, M.A., Wintle, B.A., 2013. Hydroperiod is the main driver of the spatial pattern of dominance in mangrove communities. Glob. Ecol. Biogeogr. 22, 806–817. https://doi.org/10.1111/geb.12063.

de Carvalho, Gomes F, Godoy, J.M., Godoy, M.L.D., De Carvalho, Z.L., Lopes, R.T., Sanchez-Cabeza, J.-A., Osvath, I., De Lacerda, L.D., 2011. Geochronology of anthropogenic radionuclides in Ribeira Bay sediments, Rio de Janeiro, Brazil. J. Environ. Radioact. 102, 871–876. https://doi.org/10.1016/j.jenvrad.2011.04.013.

Donato, D.C., Kauffman, J.B., Murdiyarso, D., Kurnianto, S., Stidham, M., Kanninen, M., 2011. Mangroves among the most carbon-rich forests in the tropics. Nat. Geosci. 4, 293–297. https://doi.org/10.1038/ngeo1123.

Draper, F.C., Roucoux, K.H., Lawson, I.T., Mitchard, E.T., Coronado, E.N.H., Lähteenoja, O., Montenegro, L.T., Sandoval, E.V., Zaráte, R., Baker, T.R., 2014. The distribution and amount of carbon in the largest peatland complex in Amazonia. Environ. Res. Lett. 9 (12), 124017. https://doi.org/10.1088/1748-9326/9/12/124017.

Duarte, C.M., Losada, I.J., Hendriks, I.E., Mazarrasa, I., Marbà, N., 2013. The role of coastal plant communities for climate change mitigation and adaptation. Nat. Clim. Change 3 (11), 961–968. https://doi.org/10.1038/Nclimate1970.

Duke, N., Ball, M., Ellison, J., 1998. Factors influencing biodiversity and distributional gradients in mangroves. Global Ecol. Biogeogr. Lett. 7, 27–47. https://doi.org/10.2307/2997695.

Fatem, S., Sykora, K., 2013. Vegetation of lowland tropical forest (West Papua), Human pressure, food availability and wallaby (*Dorcopsis muelleri*) presence. BIOTROPIA-Southeast Asian J. Trop. Biol. 19 (2).

Fourqurean, J., Johnson, B., Kauffman, J.B., Kennedy, H., Lovelock, C.E., et al., 2014. Field sampling of soil carbon pools in coastal ecosystems. In: Howard, J., Hoyt, S., Isensee, K., Pidgeon, E., Telszewski, M. (Eds.), Coastal Blue Carbon: Methods for Assessing Carbon Stocks and Emissions Factors in Mangroves, Tidal Salt Marshes, and Seagrass Meadows. Conservation International, Intergovernmental Oceanographic Commission of UNESCO, International Union for Conservation of Nature, Arlington, Virginia, USA, pp. 39–66.

Fourqurean, J.W., Moore, T.O., Fry, B., Hollibaugh, J.T., 1997. Spatial and temporal variation in C: N: P ratios, δ15N, and δ13C of eelgrass Zostera marina as indicators of ecosystem processes, Tomales Bay, California, USA. Mar. Ecol. Prog. Ser. 157, 147–157.

Ginting, L., Pye, O., 2013. Resisting agribusiness development: The Merauke integrated food and energy estate in West Papua, Indonesia. Austr. J. South-East Asian Stud. 6, 160–182.

Giri, C., Ochieng, E., Tieszen, L.L., Zhu, Z., Singh, A., Loveland, T., Masek, J., Duke, N., 2011. Status and distribution of mangrove forests of the world using earth observation satellite data. Glob. Ecol. Biogeogr. 20, 154–159. https://doi.org/10.1111/j.1466-8238.2010.00584.x.

Hamilton, S.E., Casey, D., 2016. Creation of a high spatio-temporal resolution global database of continuous mangrove forest cover for the 21st century (CGMFC-21). Glob. Ecol. Biogeogr. 25 (6), 729–738. https://doi.org/10.1111/geb.12449.

Houghton, R.A., 2003. The contemporary carbon cycle. Treatise Geochem. 8, 473–513.

Howard, J., Sutton-Grier, A., Herr, D., Kleypas, J., Landis, E., McLeod, E., Pidgeon, E., Simpson, S., 2017. Clarifying the role of coastal and marine systems in climate mitigation. Front. Ecol. Environ. 15, 42–50. https://doi.org/10.1002/fee.1451.

Geraldi, N.R., Ortega, A., Serrano, O., Macreadie, P.I., Lovelock, C., Krause-Jensen, D., Kennedy, H.A., Lavery, P.S., Pace, M.L., Kaal, J., Duarte, C.M., 2019. Fingerprinting blue carbon: Rationale and tools to determine the source of organic carbon in marine depositional environments. Front. Mar. Sci. 6, 263. https://doi.org/10.3389/fmars.2019.00263.

Government of Indonesia. 2016. First nationally determined contribution Republic of Indonesia. Government of Indonesia, p. 19.

Jobbágy, E.G., Jackson, R.B., 2000. The vertical distribution of soil organic carbon and its relation to climate and vegetation. Ecol. Appl. 10, 423–436.

Keith, H., Mackey, B.G., Lindenmayer, D.B., 2009. Re-evaluation of forest biomass carbon stocks and lessons from the world's most carbon-dense forests. PNAS 106 (28), 11635–11640. https://doi.org/10.1073/pnas.0901970106.

Kennedy, H., Beggins, J., Duarte, C.M., Fourqurean, J.W., Holmer, M., Marbà, N., Middelburg, J.J., 2010. Seagrass sediments as a global carbon sink: isotopic constraints. Global Biogeochem. Cycles 24 (4). https://doi.org/10.1029/2010gb003848.

Komada, T., Anderson, M.R., Dorfmeier, C.L., 2008. Carbonate removal from coastal sediments for the determination of organic carbon and its isotopic signatures, $\delta^{13}C$ and $\delta^{14}C$: comparison of fumigation and direct acidification by hydrochloric acid. Limnol. Oceanogr. Methods 6, 254–262.

Krauss, K., Allen, J., Cahoon, D., 2003. Differential rates of vertical accretion and elevation change among aerial root types in Micronesian mangrove forests. Estuar. Coast. Shelf Sci. 56, 251–259. https://doi.org/10.1016/S0272-7714(02)00184-1.

Krauss, K.W., Doyle, T.W., Twilley, R.R., Rivera-Monroy, V.H., Sullivan, J.K., 2006. Evaluating the relative contributions of hydroperiod and soil fertility on growth of south Florida mangroves. Hydrobiologia 569, 311–324. https://doi.org/10.1007/s10750-006-0139-7.

Krauss, K.W., Keeland, B.D., Allen, J.A., Ewel, K.C., Johnson, D.J., 2007. Effects of season, rainfall, and hydrogeomorphic setting on mangrove tree growth in Micronesia. Biotropica 39, 161–170. https://doi.org/10.1111/j.1744-7429.2006.00259.x.

Krauss, K.W., McKee, K.L., Lovelock, C.E., Cahoon, D.R., Saintilan, N., Reef, R., Chen, L., 2014. How mangrove forests adjust to rising sea level. New Phytol. 202, 19–34. https://doi.org/10.1111/nph.12605.

Kristensen, E., Bouillon, S., Dittmar, T., Marchand, C., 2008. Organic carbon dynamics in mangrove ecosystems: a review. Aquat. Bot. 89 (2), 201–219. https://doi.org/10.1016/j.aquabot.2007.12.005.

Kristensen, E., 2008. Mangrove crabs as ecosystem engineers; with emphasis on sediment processes. J. Sea Res. 59 (1–2), 30–43.

Kusmana, C., Onrizal, Sudarmadji, 2003. Jenis–jenis pohon mangrove di Teluk Bintuni. Fakultas Kehutaan IPB dan PT. Bintuni Utama Murni Wood Industries, Bogor.

Kusumaningtyas, M.A., Hutahaean, A.A., Fischer, H.W., Pérez-Mayo, M., Pittauer, D., Jennerjahn, T.C., 2019. Variability in the organic carbon stocks, sources, and accumulation rates of Indonesian mangrove ecosystems. Estuar. Coast. Shelf Sci. 218, 310–323. https://doi.org/10.1016/j.ecss.2018.12.007.

Labrière, N., Locatelli, B., Laumonier, Y., Freycon, V., Bernoux, M., 2015. Soil erosion in the humid tropics: a systematic quantitative review. Agric. Ecosyst. Environ. 203, 127–139.

Lamb, A.L., Wilson, G.P., Leng, M.J., 2006. A review of coastal paleoclimate and relative sea-level reconstructions using δ13C and C/N ratios in organic material. Earth Sci. Rev. 75, 29–57. https://doi.org/10.1016/j.earscirev.2005.10.003.

Lewis, R.R., 2005. Ecological engineering for successful management and restoration of mangrove forests. Ecol. Eng. 24, 403–418. https://doi.org/10.1016/j.ecoleng.2004.10.003.

Lubis, A.A., 2013. Constant rate of supply (CRS) model for determining the sediment accumulation rates in the coastal area using 210Pb. J. Coast. Develop. 10, 9–18.

Mabit, L., Gibbs, M., Mbaye, M., Meusburger, K., Toloza, A., Resch, C., Klik, A., Swales, A., Alewell, C., 2018. Novel application of Compound Specific Stable Isotope (CSSI) techniques to investigate on-site sediment origins across arable fields. Geoderma 316, 19–26. https://doi.org/10.1016/j.geoderma.2017.12.008.

MacKenzie, R.A., Foulk, P.B., Klump, J.V., Weckerly, K., Purbospito, J., Murdiyarso, D., Donato, D.C., Nam, V.N., 2016. Sedimentation and belowground carbon accumulation rates in mangrove forests that differ in diversity and land use: a tale of two mangroves. Wetlands Ecol. Manage. 24, 245–261. https://doi.org/10.1007/s11273-016-9481-3.

Marchio, D., Savarese, M., Bovard, B., Mitsch, W., 2016. Carbon sequestration and sedimentation in mangrove swamps influenced by hydrogeomorphic conditions and urbanization in Southwest Florida. Forests 7, 116. https://doi.org/10.3390/f7060116.

McKee, K.L., 2011. Biophysical controls on accretion and elevation change in Caribbean mangrove ecosystems. Estuar. Coast. Shelf Sci. 91, 475–483. https://doi.org/10.1016/j.ecss.2010.05.001.

Mcleod, E., Chmura, G.L., Bouillon, S., Salm, R., Björk, M., Duarte, C.M., Lovelock, C.E., Schlesinger, W.H., Silliman, B.R., 2011. A blueprint for blue carbon: toward an improved understanding of the role of vegetated coastal habitats in sequestering CO_2. Frontiers in Ecology and the Environment 9 (10), 552–560. https://doi.org/10.1890/110004.

Murdiyarso, D., Purbopuspito, J., Kauffman, J.B., Warren, M.W., Sasmito, S.D., Donato, D.C., Manuri, S., Krisnawati, H., Taberima, S., Kurnianto, S., 2015. The potential of Indonesian mangrove forests for global climate change mitigation. Nat. Clim. Change 5, 1089–1092. https://doi.org/10.1038/nclimate2734.

Parnell, A.C., Inger, R., 2016. Stable Isotope Mixing Models in R with simmr. URL https://cran.r-project.org/web/packages/simmr/vignettes/simmr.html.

Parnell, A.C., Inger, R., Bearhop, S., Jackson, A.L., 2010. Source partitioning using stable isotopes: coping with too much variation. PLoS ONE 5, e9672. https://doi.org/10.1371/journal.pone.0009672.

Pérez, A., Libardoni, B.G., Sanders, C.J., 2018. Factors influencing organic carbon accumulation in mangrove ecosystems. Biol. Lett. 14 (10). https://doi.org/10.1098/rsbl.2018.0237.

Perillo, G.M., Wolanski, E., Cahoon, D.R., Brinson, M.M., 2009. Coastal Wetlands: An Integrated Ecosystem Approach. Elsevier.

Phillips, D.L., Inger, R., Bearhop, S., Jackson, A.L., Moore, J.W., Parnell, A.C., Ward, E.J., et al., 2014. Best practices for use of stable isotope mixing models in food-web studies. Can. J. Zool. 92 (10), 823–835. https://doi.org/10.1139/cjz-2014-0127.

Pregitzer, K.S., Euskirchen, E.S., 2004. Carbon cycling and storage in world forests: biome patterns related to forest age. Glob. Change Biol. 10, 2052–2077. https://doi.org/10.1111/j.1365-2486.2004.00866.x.

Ranjan, R.K., Routh, J., Ramanathan, A.L., Klump, J.V., 2011. Elemental and stable isotope records of organic matter input and its fate in the Pichavaram mangrove–estuarine sediments (Tamil Nadu, India). Mar. Chem. 126, 163–172. https://doi.org/10.1016/j.marchem.2011.05.005.

R Core Team, 2018. R: A language and environment for statistical computing. R Foundation for Statistical Computing, Vienna, Austria. https://www.R-project.org/.

Reef, R., Feller, I.C., Lovelock, C.E., 2010. Nutrition of mangroves. Tree Physiol. 30, 1148–1160. https://doi.org/10.1093/treephys/tpq048.

Richards, D.R., Friess, D.A., 2016. Rates and drivers of mangrove deforestation in Southeast Asia, 2000–2012. PNAS 113 (2), 344–349. https://doi.org/10.1073/pnas.1510272113.

Robertson, A.I., 1991. Plant-animal interactions and the structure and function of mangrove forest ecosystems. Aust. J. Ecol. 16 (4), 433–443.

Rosentreter, J.A., Maher, D.T., Erler, D.V., Murray, R.H., Eyre, B.D., 2018. Methane emissions partially offset "blue carbon" burial in mangroves. Science. Advances 4, eaao4985. https://doi.org/10.1126/sciadv.aao4985.

Rouw, A., Hadi, T.W., HK BT, Hadi, S., 2014. Analisis variasi geografis pola hujan di Wilayah Papua. Jurnal Tanah dan Iklim 38, 25-34.

Ryba, S.A., Burgess, R.M., 2002. Effects of sample preparation on the measurement of organic carbon, hydrogen, nitrogen, sulfur, and oxygen concentrations in marine sediments. Chemosphere 48 (1), 139–147.

Samper-Villarreal, J., Lovelock, C.E., Saunders, M.I., Roelfsema, C., Mumby, P.J., 2016. Organic carbon in seagrass sediments is influenced by seagrass canopy complexity, turbidity, wave height, and water depth. Limnol. Oceanogr. 61, 938–952. https://doi.org/10.1002/lno.10262.

Sanchez-Cabeza, J., Masqué, P., Ani-Ragolta, I., Merino, J., Frignani, M., Alvisi, F., Palanques, A., Puig, P., 1999. Sediment accumulation rates in the southern Barcelona continental margin (NW Mediterranean Sea) derived from 210Pb and 137Cs chronology. Prog. Oceanogr. 44, 313–332.

Sanchez-Cabeza, J., Ruiz-Fernández, A., 2012. 210Pb sediment radiochronology: an integrated formulation and classification of dating models. Geochim. Cosmochim. Acta 82, 183–200.

Sanders, C.J., Smoak, J.M., Naidu, A.S., Sanders, L.M., Patchineelam, S.R., 2010. Organic carbon burial in a mangrove forest, margin and intertidal mud flat. Estuar. Coast. Shelf Sci. 90, 168–172. https://doi.org/10.1016/j.ecss.2010.08.013.

Saragi-Sasmito, M.F., Murdiyarso, D., June, T., Sasmito, S.D., 2018. Carbon stocks, emissions, and aboveground productivity in restored secondary tropical peat swamp forests. Mitig. Adapt. Strat. Glob. Change 24 (4), 521–533. https://doi.org/10.1007/s11027-018-9793-0.

Sasmito, S., Kuzyakov, Y, Lubis, A.A., Murdiyarso, D., Hutley, L., Bachri, S., Friess, D.A., Martius, C., Borchard, N., 2019. SWAMP Dataset-Mangrove carbon burial and sources-Bintuni-2019. Center for International Forestry Research (CIFOR), V2. https://doi.org/10.17528/CIFOR/DATA.00102.

Serrano, O., Almahasheer, H., Duarte, C.M., Irigoien, X., 2018. Carbon stocks and accumulation rates in Red Sea seagrass meadows. Sci. Rep. 8, 15037. https://doi.org/10.1038/s41598-018-33182-8.

Sillanpää, M., Vantellingen, J., Friess, D.A., 2017. Vegetation regeneration in a sustainably harvested mangrove forest in West Papua, Indonesia. For. Ecol. Manage. 390, 137–146. https://doi.org/10.1016/j.foreco.2017.01.022.

Smoak, J.M., Breithaupt, J.L., Smith, T.J., Sanders, C.J., 2013. Sediment accretion and organic carbon burial relative to sea-level rise and storm events in two mangrove forests in Everglades National Park. Catena 104, 58–66. https://doi.org/10.1016/j.catena.2012.10.009.

Soper, F.M., MacKenzie, R.A., Sharma, S., Cole, T.G., Litton, C.M., Sparks, J.P., 2019. Non-native mangroves support carbon storage, sediment carbon burial, and accretion of coastal ecosystems. Glob. Change Biol. https://doi.org/10.1111/gcb.14813.

Stringer, C.E., Trettin, C.C., Zarnoch, S.J., 2016. Soil properties of mangroves in contrasting geomorphic settings within the Zambezi River Delta, Mozambique. Wetlands Ecol. Manage. 24, 139–152. https://doi.org/10.1007/s11273-015-9478-3.

Sukardjo, S., Alongi, D.M., Kusmana, C., 2013. Rapid litter production and accumulation in Bornean mangrove forests. Ecosphere 4, art79. https://doi.org/10.1890/es13-00145.1.

Thornton, S., McManus, J., 1994. Application of organic carbon and nitrogen stable isotope and C/N ratios as source indicators of organic matter provenance in estuarine systems: evidence from the Tay Estuary, Scotland. Estuar. Coast. Shelf Sci. 38, 219–233.

Twilley, R.R., Rovai, A.S., Riul, P., 2018. Coastal morphology explains global blue carbon distributions. Front. Ecol. Environ. 16 (9), 503–508. https://doi.org/10.1002/fee.1937.

Wahyudi, A.J., Afdal, 2019. The origin of the suspended particulate matter in the seagrass meadow of tropical waters, an evidence of the stable isotope signatures. Acta Oceanol. Sin. 38, 136–143. https://doi.org/10.1007/s13131-019-1380-z.

Weiss, C., Weiss, J., Boy, J., Iskandar, I., Mikutta, R., Guggenberger, G., 2016. Soil organic carbon stocks in estuarine and marine mangrove ecosystems are driven by nutrient colimitation of P and N. Ecol. Evol. 6, 5043–5056. https://doi.org/10.1002/ece3.2258.

Werth, M., Mehltreter, K., Briones, O., Kazda, M., 2015. Stable carbon and nitrogen isotope compositions change with leaf age in two mangrove ferns. Flora – Morphol. Distrib. Funct. Ecol. Plants 210, 80–86. https://doi.org/10.1016/j.flora.2014.11.001.

Woodroffe, C.D., Rogers, K., McKee, K.L., Lovelock, C.E., Mendelssohn, I.A., Saintilan, N., 2016. Mangrove sedimentation and response to relative sea-level rise. Ann. Rev. Mar. Sci. 8, 243–266. https://doi.org/10.1146/annurev-marine-122414-034025.

Xiong, Y., Liao, B., Wang, F., 2018. Mangrove vegetation enhances soil carbon storage primarily through in situ inputs rather than increasing allochthonous sediments. Mar. Pollut. Bull. 131, 378–385. https://doi.org/10.1016/j.marpolbul.2018.04.043.